

Natural convection heat transfer enhancement of aluminum heat sink using Nano coating by electron beam method

Senthil kumar Pongiannan^{a*}, Velraj Ramalingam^b, Latha Nagendran^a

^aAU-FRG Institute for CAD/CAM, College of Engineering, Anna University, Chennai-600 025, India.

^bInstitute for Energy Studies, College of Engineering, Anna University, Chennai-600 025, India.

*Corresponding Author E-mail address: erodesenthil@yahoo.com

The high power density and compactness of the next generation electronic devices necessitate efficient and effective cooling methods for heat dissipation in order to maintain the temperature at an acceptable safety level. In the present work, aluminum nano coating was employed in a heat sink to study the heat transfer performance under natural convection conditions. The nano-coating was achieved using an Electron beam method while the characteristics of nano-coated surfaces were analysed using scanning electron microscopy, an energy dispersive X-ray spectroscopy, surface roughness profilometry equipment and by X-ray diffraction techniques. The heat dissipation from heat sink with and without Nano coating under natural convection has been experimentally studied at different controllable surrounding temperatures. A uniform increase in the surface roughness by the nano-coating was seen in all cases. The conclusion from several experimental results was that the effect of nano-coating in augmenting the heat transfer is more pronounced only when there is a sufficient temperature driving potential.

Key words: Heat sink; Nano-coating; Heat transfer enhancement; EDS; surface roughness; Natural convection

1. Introduction

The accelerating pace of discovery and innovation in the electronic industries has led to an exponential increase in power densities, which, in turn, drive the innovation of smarter and smaller products. The tremendous growth in electronic equipment in which nearly 80-90% of the energy is converted into heat demands pioneering solutions to the new challenges of thermal management. The main challenges on the thermal management front can be understood by the heat dissipation of electronic devices, which vary from 5 W.cm⁻² to 2000 W.cm⁻².

Michael Pecht [1] reports that 55% of the failures in electronics are due to overheating and 20% due to vibration, 6% due to dust and 19% due to humidity. Hence, thermal management is essential in electronic industries, as it improves reliability and enhances performance through effective removal of the

heat generated by the devices. The generation of heat may cause inaccuracies and sometimes lead to system failures. So, in consumer electronic industries, semiconductor devices are often specified with operating temperature range from 0 to 70°C [2&3]. Su Jingxin [4] have noted the rapid acceleration in the global demand for reliable, efficient and economic heat exchanging equipment used in power and process industries, medical devices etc., with better airside heat transfer performance and great improvements in energy conservation and protection of the environment. Farhad Sarvar et al. [5] have stated that any metal surface has roughness due to infinitesimal hills, valleys and poor surface texture or surface topography. The surface between the electronic components is separated by a layer of interstitial air. These gaps are filled with low thermal conductivity of air that reduces the heat transfer to a great extent. Considering the above, researchers have taken up various studies with theoretical and experimental focus for enhancing heat transfer. Starner and McManus [6] have done experimental investigation of the average heat transfer coefficient of horizontal surfaces with rectangular fin arrays for various sink orientation and dimensions. The heat transfer rate for horizontal orientation has been proved to be more favorable than others. Jones and Smith [7] have done investigation experiments on the average heat transfer coefficient over a wide range of horizontal arrays and arrived at the optimum fin spacing for maximum heat transfer from a given base surface. Li and Chao [8] did variations in the plate-fin heat sinks fin height, width, and the Reynolds number to investigate their thermal performance. The highest fin had the best thermal performance of the heat sink with a constant width. For a certain value of Reynolds number at a constant fin height, width improves thermal performance and, after a certain value, the pressure drop increases with increase in the height, width and Reynolds number. In electronic cooling, pin fins are widely used for getting increased cooling. The analytical, numerical analysis and experimental thermal performance and overall convective heat transfer coefficient studies on pin-fin have been reported by Kobus et al. and Ricci et al. [9-10]. Selection and optimization of the pin fin cross-section for electronics cooling were carried out by Sahiti et al. [11] and their studies show elliptical cross section providing better heat exchanger performance.

In industries, the importance of new material coatings has resulted in a remarkable enhancement of innovation in thin film coating technology. Recent literature shows the nano coating on the surface resulting in an appreciable enhancement in heat transfer. Shanmugan and Mutharasu [12] coated 400nm thickness of Aluminum Nitride (AlN) on copper (Cu) substrate using direct current (DC) sputtering for application of thermal interface material (TIM). They report a reduction in junction temperature and thermal resistance when compared with non-coated Cu substrate. Schowalter et al. [13] indicate the use of AlN as substrate for electronics applications. Dietz and Joshi [14] have done a comparative experimental study of the role of heat removal in electronic cooling applications by growing carbon nanotubes (CNT) on the bottom surface of silicon microchannel. Senthilkumar et al. [15] coated carbon nanotubes on the brass extended surfaces. The heat transfer characteristics were investigated using the Taguchi method for the experimental design. The performances of coated and non-coated rectangular brass fins were compared. The average percentage increase in heat transfer rate was seen to be around 12%. Senthilkumar et al. [16] have chosen rectangular aluminum fins coated with carbon nanotubes for analysis using the physical vapor deposition (PVD) method for enhancing the fin heat transfer rate.

Convective heat transfer rates for coated and non-coated surfaces were calculated and compared. A 5% improvement in the average percentage in fin efficiency for carbon nano coated aluminum surfaces was found. Yao et al. [17] fabricated uniform silicon nanowire (Si NW) structures on the top, bottom and sidewall surfaces of the microchannel heat sinks using the two-step electroless etching process. The micro/nano hierarchical structure was found to yield a superior boiling heat transfer performance. An improvement in the maximum heat flux by 150% over the microchannel heat sinks and 400% over the plain silicon surface was seen. Lotfizadeh et al. [18] have studied the thermal performance of innovative heat sinks using metallic foams and aluminum nanoparticles. They found a better performance from thermal resistance of heat sinks with aluminum nanoparticle than from the other heat sinks considered for comparison since metallic foam heat sinks are expensive and have a large dirt absorbing property. Yakut Ali et al. [19] did experimental investigation of the single phase heat transfer and pressure drop characteristics for shallow rectangular microchannel heat sink. They observed the Copper nanowires coated heat sink temperature as lower compared to bare microchannel heat sinks at each thermocouple location under the same power input and flow rate. Hence, an attempt has been made in the present work to study the technological importance and the recent growth in cooling systems for electronic devices for enhancement of performance using nano-coated heat sinks. The main objectives are to prepare a nano-coated heat sink using the beam evaporation method, to study the characteristics of the surface and to compare the heat transfer performance enhancement of the nano-coated heat sink with non-coated heat sink under natural convection conditions.

2. Materials and Methods

2.1. Preparation of nano-coated heat sink

In the present work, aluminum pin-fin heat sink used in the existing computer configuration, HP XW 4300 workstation was identified for the investigation of the heat transfer performance enhancement through nano-coating. Figure 1 is the photographic view of the heat sink. The dimensions of the heat sink are detailed in tab.1. The Electron Beam (EB) evaporation technique which is one type of Physical vapor deposition (PVD) used for nano-coating. DC Box-type vacuum coating machine procured from Hind High Vacuum, Bangalore, India was used for the coating.

Table 1. Dimensions of the heat sink

Base area	42.5×42.5	mm ²
Base Thickness	3.5	mm
Fin Height	26.5	mm
Fin width	3.5	mm
Transverse pitch	2.07	mm
Longitudinal pitch	2.77	mm
No. of Fins	96	Nos.
Total exposed area	27103.5	mm ²

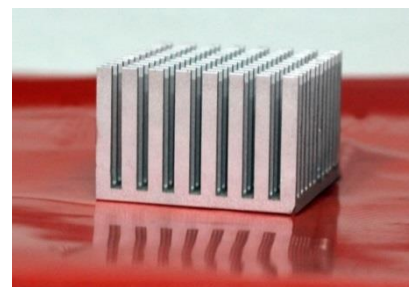


Figure 1. Photographic view of aluminum heat sink

Aluminum nano powder with an average size of 400-800nm with 99.90% purity procured from Nano labs-Jamshedpur was chosen for coating. Nano-powder was used for preparing a target aluminum pellet of size 25mm diameter and 10mm height using a hydraulic press. The aluminum substrate on which coating was to be performed was washed using neutral soap solution and subsequently cleaned with acetone (15 minutes) and distilled water (15 minutes) in an ultrasonic bath and then dried and placed in a vacuum chamber.

An electric power supply with a voltage of 10kV was passed through a tungsten filament and the pellet was heated to the level where thermionic emission of electrons occurred. The electron beam cause evaporation of the atoms from the target material to gaseous phase coating all sides of the Al substrate under typically 10E-5Torr vacuum pressure. The average working distance between the target and substrate was 400mm. Deposits of uniform microstructure aluminum single layer coating of 400nm thickness were seen on the Al substrate. The advantage with this process was the achievement of uniform coating and precise layer monitoring. The process parameter details of the machine during the operation are given in tab. 2.

Table 2. Specifications of DC Box-type vacuum coating machine during operation

Base Pressure	3×10^{-5}	Torr
Working Pressure	5×10^{-4}	Torr
Target-Substrate distance	400	mm
Substrate Temperature	350	°C
Duration	120	mins

2.2 Surface characterization study (Surface topography)

The surface morphology and the chemical composition of the non-coated and nano-coated heat sink samples were characterized using Scanning electron microscopy (SEM) along with energy dispersive X-rays spectroscopy (EDS) using a Hitachi S-3400N scanning Electron Microscope and X-ray diffraction (XRD) pattern were recorded by Bruker D2 PHASER available at Anna University, Chennai. The analysis was carried out under a secondary electron mode with an acceleration voltage of 10kV and 15kV. EDS analysis is an analytical technique used for the elemental analysis or chemical characterization of a sample. The element has a unique atomic structure allowing X-rays to characterize the elemental atomic structure and to identify the uniqueness between one another. It is used for the validation of the composition of aluminum and oxide percentage present in the samples. The surface texture of the coated and non-coated samples was measured for fine irregularities, such as peaks and valleys. It was characterized through 2D and 3D surface profiles obtained by using the Talysurf CI LITE 3D surface roughness profilometry equipment. This equipment has the non-contact roughness measurement feature with a magnification of 10x.

2.3 Experimental investigation on heat transfer performance

An experimental unit was constructed in the present work for a study of the heat transfer characteristics of the nano-coated heat sink under natural convection conditions. Figure 2 is the photographic view of the experimental setup which consisted of a duct made up of acrylic sheet, heating arrangement with auto-transformer, heat sink, temperature sensors and power measurement devices connected to a Data acquisition system. A flat plate heating element of 300W was placed on a wooden plate and kept inside a closed environment with vents on both sides. The heat sink base was mounted on a flat plate heater using an adhesive paste of high thermal conductivity to enable supply of the maximum quantity of heat to the plate to pass through the heat sink. The flat plate heater connected through a dimmerstat (autotransformer) was used for regulating the AC supply voltage and selecting the necessary heating level. The input circuit current was measured using a i310S Fluke AC/DC current clamp meter. The temperature along the height of the fin was measured using J-type (iron-constantan) thermocouples, embedded on the fin wall surface within the heat sink at one-fourth, middle, three-fourth, and the tip of the heat sink (by providing small insert hole on the fins).

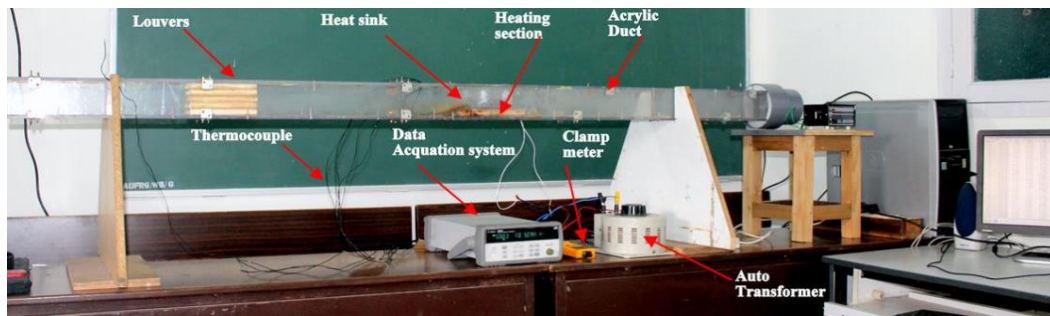


Figure 2. Photographic view of the Experimental Setup

A thermocouple was mounted between the heater and the heat sink base for measuring the base temperature by ensuring a good thermal contact. The surrounding temperature was also measured using a separate thermocouple. The uncertainty in temperature measurement was seen as $\pm 1.1^\circ\text{C}$. The instrumentation devices were interfaced with a computer through an Agilent data acquisition system which was connected to the setup for measuring temperature, voltage and current.

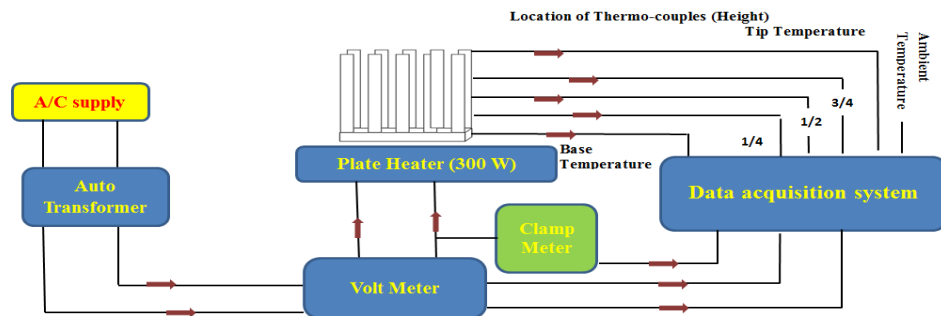


Figure 3. Schematic representation showing the measuring instruments

Figure 3 is the schematic representation of the measuring devices connected to the data acquisition system. The experiments were conducted in a large room and care was taken to maintain room temperature constant and free of air currents.

2.4 Testing technique (Operating procedure)

The experiments were conducted at Chennai, where it is possible to maintain the room temperature of building within a variation of $\pm 0.1^\circ\text{C}$ for a long duration of more than two hours under natural conditions. This is mainly due to the location of the building near the coast, where the ambient temperature is moderated in a day by a large thermal mass of the sea with the diurnal temperature variation within 6°C during most of the days in the year. Hence no separate provision was made for maintaining the surrounding temperature. The experiments were conducted when the room temperature was at the required levels.

Initially, several trial experiments were performed to assess the heat input at which the base of the heat sink with nano-coating attained a steady state temperature of 70°C when the surrounding temperature (T_∞) was 27°C . The temperature of 70°C was selected considering that most of the commercial electronic devices are designed to withstand a temperature up to 70°C [2&3]. The surrounding temperature of 27°C is the lowest temperature in the range of temperature identified (27°C to 30°C) for the conduct of experiments. The heat sink attained a steady state temperature of 70°C when the heat input was 6W for the lowest surrounding temperature of 27°C and with nano-coating. Hence, the steady state temperature was more than 70°C for all the surrounding temperatures and for the coated and non-coated conditions when a constant heat input of 6W was given.

In all the experimental trials, the heat sink was at the surrounding temperature to start with. A heat input of 6W was provided at the base of the heat sink by varying the voltage (V) using a dimmerstat. The time taken by the heat sink to reach 70°C was measured for all the experiments. The temperature variation in the heat sink along the fin height was also measured when the base of the heat sink reached 70°C . Using these temperature measurements and the time required to attain 70°C , the performance of the nano-coated heat sink was compared with that of the non-coated heat sink. Zografos and Sunderland [20] and Joo and Kim [21] found the effect of radiation as less than 5% under natural convection conditions, they suggested that the radiation effect could be neglected. The experiments were conducted also for the analysis of the performance of the heat sink when the heat input to the base was turned off from the position when the base of the heat sinks as at 70°C . In all the trial experiments the time taken by the heat sink to reach 30°C from 70°C under various constant surrounding temperature conditions was measured and the results were used for comparison of the performance of nano-coated heat sink with the non-coated heat sink.

In the present work, the uncertainty of temperature was evaluated, based on the error propagation method proposed by Strupstad [22]. HP-Agilent 34970A, Data Acquisition System (DAS) was used for recording the temperatures, at a scanning rate of 10seconds throughout the experiment. The variation in the temperature conversion accuracy of the data logger was $\pm 0.02^\circ\text{C}$. The sink temperature at each fin

location, the temperature at the base of the sink temperature and surrounding temperature were measured using six of J-type thermocouples (accuracy $\pm 1.1^{\circ}\text{C}$). The uncertainty involved in the temperature measurement was $\pm 4.18\%$.

3. Results and Discussion

The characteristics of the nano-coated surface compared to the non-coated surface obtained from the present analysis have been reported in the earlier part of this section.

3.1. EDS analysis

The EDS spectrum presented in fig. 4 relates to the non-coated and nano-coated heat sink that indicated the composition of aluminum and oxide observed in the samples. Table 3 shows the non-coated heat sink consisted of aluminum and oxides with 91.39% and 8.61% respectively whereas the nano-coated heat sink consisted of aluminum and oxide with 97.84% and 2.16% respectively.

Table 3.
Weight percentages of the elements present in the heat sinks

Element	Weight%	
	Nano-coated	Non-coated
Aluminum	97.84	91.39
Oxide	2.16	8.61

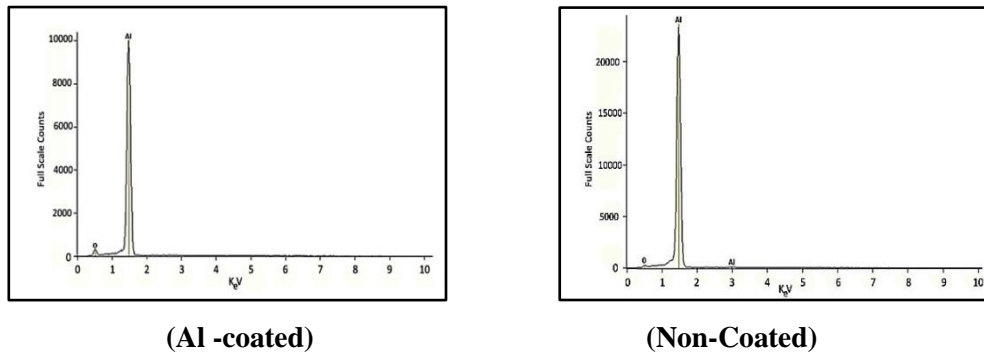
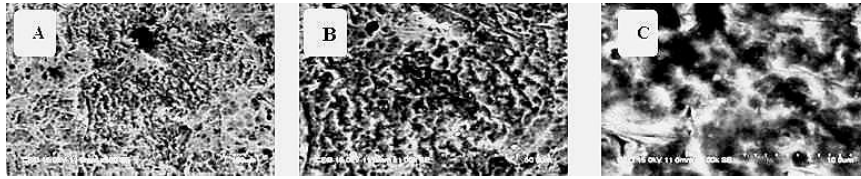


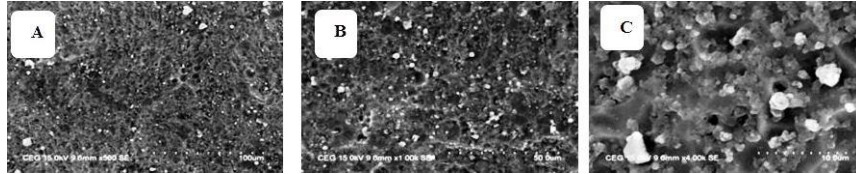
Figure 4. EDS spectrum of non-coated and Nano-coated heat sink

3.2. SEM Characterization

Figure 5 shows the SEM images of non-coated and nano-coated heat sinks with different magnification factors. These images depict surface morphology and explain the manner in which the nano particles are spread across the surfaces on the nano-coated heat sink. Figure 5 shows the uniform coating spread along the surface with the particles spherically coated in a fully covered pattern.



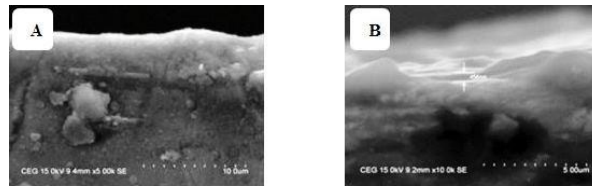
(A) 500 SE (B) 1.00 K SE (C) 5.00 K SE
(a) Non-coated



(A) 500 SE (B) 1.00 K SE (C) 4.00 K SE
(b) Nano-coated

Figure 5. SEM images of the samples

The cross-sectional SEM image of aluminum coated heat sink is shown in fig.6, and the resulting thicknesses of nano-coating ranges are seen from 400 to 500 nanometers.

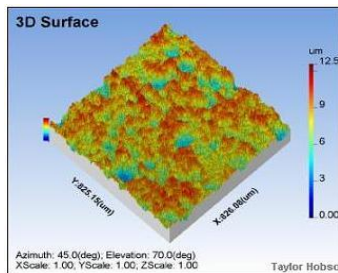


(A) 5.00 K SE (B) 10.00 K SE

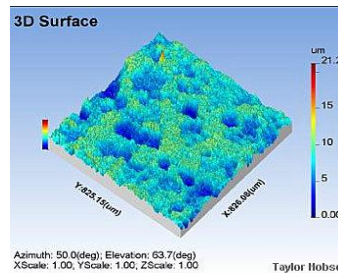
Figure 6. Cross-sectional SEM images of aluminum coated sink

3.3. Surface roughness analysis

Figure 7 shows the 3D surface topography images of non-coated and nano-coated samples produced by the 3D optical surface profiler and depicting the spread of the roughness levels along the surface of the heat sink.



(a) Non-coated



(b) Nano-coated

Figure 7. 3D Surface topography characterization

The results show the nano-coated surface having a randomized distribution of peaks and valleys over the non-coated surface. The average roughness (R_a) figures measured were $0.65\mu\text{m}$ and $0.87\mu\text{m}$ for non-coated and nano-coated samples respectively. The maximum heights (R_z) of roughness profile were $3.555\mu\text{m}$ and $5.192\mu\text{m}$ for non-coated and nano-coated sample respectively. The nano-coated heat sink was seen having a higher value of roughness compared to the non-coated heat sink. This was very useful for enhancing the heat transfer performance.

3.4. X-ray diffraction (XRD) analysis

X-ray diffraction (XRD) analysis provides information on the structural characteristics of materials like mean crystalline size and crystallinity. The patterns were recorded by Bruker D2 PHASER using CuK_α (1.5418\AA) radiation at scanning rate of $0.02^\circ/\text{s}$. Debye-Scherrer equation, the single-line approximation, and the linear fitting were used for obtaining structural information through the mathematical analysis of the XRD.

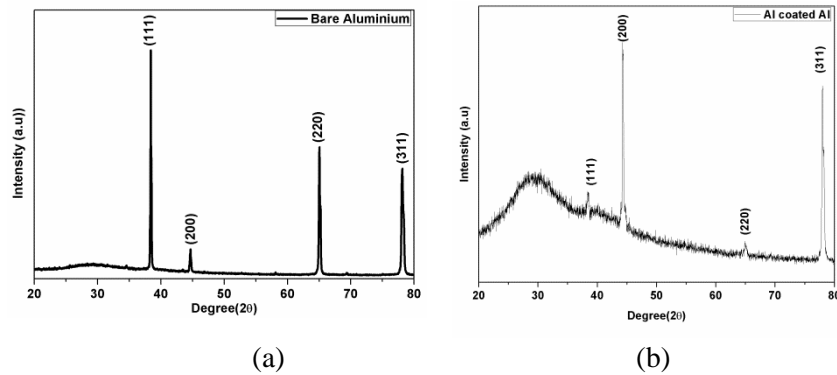


Figure 8. XRD spectra for (a) Bare aluminum (b) Aluminum coated Aluminum

XRD patterns of aluminum substrate and aluminum coated aluminum substrate are shown in the fig. 8. The diffraction patterns of both the samples are indexed using the standard XRD patterns of aluminum (JCPDS 89-4037) and that confirm the cubic structure. The sharp and intense peaks in fig. 8 (a) shows the high crystalline nature of the material with preferred orientation of (111) whereas the fig. 8 (b) Al coated Al has the preferred orientation of (200) with suppression of (111) which shows the effective coating of Al on Al substrate. The crystalline size of the coated Al layer was calculated as 60nm using Debye-Scherrer formula.

3.5. Heat transfer characteristics

The main objective of the present work is to investigate the effect of heat transfer enhancement arising from nano-coating in a heat sink under natural convection conditions. The results of the experiments conducted when the bottom of the heat sink was supplied with constant heat input condition and the system exposed to various surrounding temperature (T_∞) conditions have been presented. The results of the experiments conducted during the cooling of the heat sink when the heat input was turned

off from the prescribed maximum temperature and exposed to a convective environment with various surrounding temperature conditions are presented in later part of this section. The effectiveness of coating at various conditions was assessed and compared with the case without coating. Figure 9 (a-d) shows the temperature variations seen along the fin height for coated and non-coated heat sink when the base temperature was 70°C under various constant surrounding temperature conditions after the heat sink attained a steady state. The figure shows a continuous temperature variation from the fin base to the fin tip (T_p) at all surrounding temperatures in the case of a non-coated heat sink. However, in the case of nano-coating, the temperature at 75% of the height of the fin and fin tip was the same when the surrounding temperature was maintained at 27°C and 28°C and with only a negligible drop in temperature between the three-fourth height and fin tip when the surrounding temperature maintained was between 29°C and 30°C .

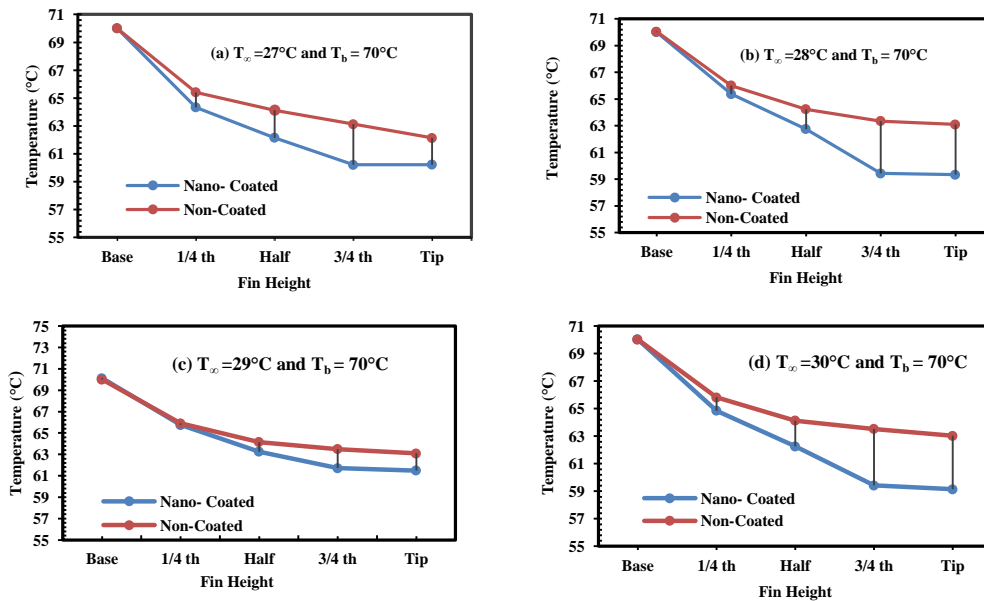


Figure 9. Temperature variation along the fin height under various constant surrounding temperatures.

(a) $T_{\infty}=27^{\circ}\text{C}$

(b) $T_{\infty}=28^{\circ}\text{C}$

(c) $T_{\infty}=29^{\circ}\text{C}$

(d) $T_{\infty}=30^{\circ}\text{C}$

It is inferred from the above temperature distribution along the height of the fin that there was no heat transfer from the top 25% of the fin height through the lateral surface in the case of nano-coated heat sink. The higher heat transfer coefficient in the case of nano-coated heat sink due to increased surface roughness (from $0.65\mu\text{m}$ to $0.87\mu\text{m}$), transferred the entire heat from the fin base within the 75% of the fin height even after the system attained a steady state. However in the case of non-coated heat sink, the temperature variation existed till the fin tip showed the transfer of heat by utilizing the entire surface area of the fin. Hence it is construed that the fin height could be reduced by 25% in the case of nano-coated heat sink particularly at a lower surrounding temperature for achieving the same heat transfer as in the non-coated heat sink.

Figure 10 is an approximate representation of the thermal boundary layer developed near the walls of two adjacent fins on the basis of the temperatures measured under steady state conditions shown in the fig. 9. for both the non-coated and nano-coated heat sinks. In both cases, a constant heat input of 6W was provided and the experiments were conducted for two different surrounding temperatures of 27°C and at 30°C. Figure 10(a) and 10(b) shows the variation in the boundary layer development under 27°C and 30°C for the non-coated and nano-coated heat sink respectively. When the surrounding temperature was lower (27°C), the air density was high and hence the volume occupied by the free stream air was more between the fins. However, when the surrounding temperature was higher (30°C), the prevailing lower density of the air resulted in the free stream air occupying a minimal volume between the fins. It is a well-known fact that when the thermal boundary layer thickness is small, heat transfer rate is maximum. The higher temperature drop along the top one-fourth height of the fin in the non-coated heat sink at 27°C compared to 30°C (fig. 9 (a) and (d)) show that the heat transfer from the top one-fourth height of the fin should be higher at 27°C compared to 30°C. This is represented with a thinner boundary layer thickness in the case of 27°C compared to 30°C. Hence the reduction in the surrounding temperature has a significant effect in augmenting the heat transfer.

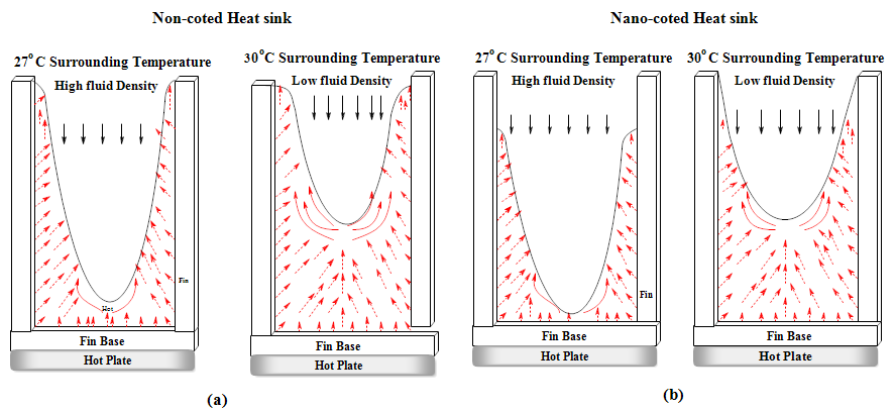


Figure 10. Nano-coated and Non-coated heat sinks

In the case of nano-coated heat sink, there is no temperature variation in the top one-fourth height of the fin. The inference from fig. 10. is that there is no heat transfer from this portion of the fin. This is due to the entire heat from the base of the heat sink transferred through three-fourth of the height of fin as the increased surface roughness of the nano-coated heat sink does not allow the growth of the boundary layer that increases the heat transfer rate. Hence, the start of boundary layer was shown only from one-fourth of height from the tip of the fin. However, in the case of nano-coating with 30°C surrounding temperature, a small temperature drop was seen along the one-fourth height of the fin from the tip which showed a marginal heat transfer in that region and represented by a very small boundary layer development near the fin tip.

Figure11 shows the time required for the heat sink to attain a temperature of 70°C when the heat input at the base of the heat sink was 6W and the surrounding temperature was maintained at a constant uniform temperature at various discrete temperature levels between 27°C to 30°C. Figure 11 shows the

requirement of the nano-coated heat sink to reach 70°C as 76 minutes when the surrounding temperature was maintained at 27°C, whereas the non-coated heat sink attained the same temperature within 35 minutes. A 117% increase in the time required in the nano-coated heat sink compared to the non-coated heat sink was shown. However, there was a decrease in the percentage enhancement of the time required in the nano-coated heat sink with the increasing the surrounding temperature. The enhancement was only 14% when the surrounding temperature was maintained at 30°C. In both the cases of non-coated and nano-coated heat sinks, an appreciable decrease in the time required for the heat sink to attain 70°C was seen despite only a small increase in the surrounding temperature. The decrease in heat transfer was appreciable following an increase in the surrounding temperature as the heated air surrounding the heat sink was not moving easily from the space between the fins due to natural convection. Hence the effective surrounding temperature was very high and attaining very close to the heat sink surface temperature. This necessitated only a driving potential for the dissipation of the heat than the surface modification that enhanced the heat transfer coefficient. The above results demonstrate the predominant influence of the surrounding temperature compared to the effect of nano-coating. However the nano-coating that enhances the surface heat transfer coefficient due to increased roughness plays a vital role when there is sufficient temperature driving potential.

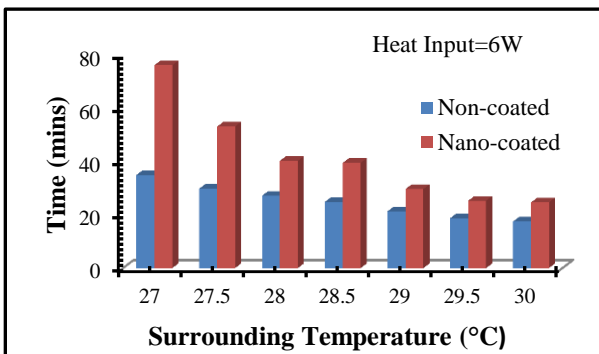


Figure 11. Time taken for the heat sinks to attain 70°C under various constant surrounding temperatures

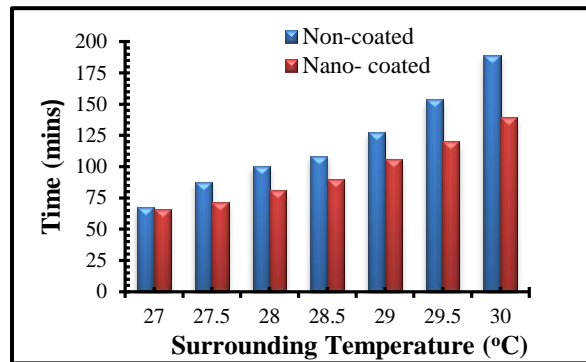


Figure 12. Time taken by the heat sinks to reach 30°C from 70°C under various constant surrounding temperatures.

Figure 12 shows the results of the experiments conducted with natural cooling of the heat sink from the prescribed maximum temperature of 70°C to 30°C with the ambience maintained at a constant uniform temperature at various levels for both the cases of nano-coated and non-coated heat sinks. The figure shows that when the surrounding temperature was maintained at 27°C, the effect of nano-coating was not distinct, and that the temperature driving potential had the predominant effect compared to the convective heat transfer coefficient and the exposed surface area. However, when the surrounding temperature was increased, there was a marginal effect due to nano-coating and this increasing effect was more predominant at the highest temperature of 30°C. When the surrounding temperature was maintained at 30°C, the time required for reducing the heat sink from 70°C to 30°C was less by 26% in the case of nano-coated heat sink compared to the non-coated heat sink.

The results obtained during the heating and cooling of the heat sink showed a contradictory effect in the performance enhancement due to nano-coating, with variation in surrounding temperature of the heat sink. During the heating of the heat sink, the nano-coating showed enhanced performance with decrease in surrounding temperature while the nano-coating showed increased performance during the cooling of the heat sink with increase in surrounding temperature.

When the heat sink was heated, the temperature of the surrounding air at the immediate vicinity of the heat sink was increased with respect to time. At this juncture, as the surrounding air temperature was higher, the heated air with lower density moved up easily. The increase in the surface roughness due to nano-coating disrupts the growth and reduces the thickness of the boundary layer contributing for the enhancement in heat transfer. When the temperature of the surrounding air is decreased, owing to the higher density, it did not allow easy movement of the heated air from the fin surface. In the case of cooling, the temperature of the surrounding air at the immediate vicinity of the heat sink is decreased with respect to time. At this juncture, when the temperature of the surrounding air was lower, the air moved down replacing the air near the immediate vicinity of the sink. As the temperature of the surrounding air increased with lower density, it could not move downward easily to replace the air near the immediate vicinity of the heat sink. Hence there was a difficulty for the air in flowing downward with increase in the temperature of the surrounding air. The nano-coating provided on the heat sink enhances the heat transfer by disrupting the growth of the boundary layer and the effect was more pronounced when there was an increase in the temperature of the surrounding air.

4. Conclusions

This work presents the preparation of a nano-coated heat sink through the use of the electron beam method, surface characterization and heat transfer performance enhancement during cooling and heating of the heat sink when exposed to various constant surrounding temperature conditions under natural convection.

The key findings from the present work are (i) The EDS spectrum indicates increase in the aluminum weight percentage in the nano-coated surface from 91.39% to 97.84% and a decrease in the oxide weight percentage from 8.61% to 2.16%. (ii) The SEM image depicts uniformity in the distribution of the coating along the surface and the nanoparticles had a spherical shape covering the entire surface. The range of thickness of nano-coating was from 400nm to 500nm. (iii) The average surface roughness increased from 0.65 μm (Ra) to 0.87 μm (Ra) due to nano-coating. (iv) There was no temperature variation in the upper one-fourth height of the fin when a constant heat input of 6W was provided in the nano-coated heat sink. Hence it is inferred that the fin height could be reduced by 25% in the case of the nano-coated heat sink for achieving the equivalent heat transfer performance. (v) During the heating of the heat sink, enhancement in performance increased with decrease in surrounding temperature, and during the cooling of the heat sink, the enhancement in performance increased with increase in surrounding temperature, as a result of nano-coating. (vi) The nano-coating that enhances the surface heat transfer coefficient due to increased roughness plays a vital role only when there is sufficient temperature driving potential.

Nomenclature

H	- Fin height, [mm]
N	- Number of fins
A	- Surface area of sink, [mm ²]
T	- Temperature, [°C]
T _∞	- Ambient temperature, [°C]
T _b	- Base temperature, [°C]
T _p	- Tip temperature, [°C]
ΔT	- Temperature difference, [°C]
k	- Thermal conductivity, [Wm ⁻¹ .K ⁻¹]
t	- Time, [mins]
W	- Watts
V	- Voltage
P	- Pressure, [Torr]
Q	- Heat transfer rate, [W]

Abbreviation

PVD	- Physical vapor deposition
EB	- Electron Beam
SEM	- Scanning electron microscopy
EDS	- Energy dispersive analysis of X-rays spectroscopy
SE	- Secondary electron
XRD	- X-ray diffraction

Subscripts

b	- Base
∞	- Ambient
a	- Arithmetic mean deviation
z	- Maximum height
P	- Tip

References

- [1] Michal Pecht, Handbook of electronic package design, Marcel Dekker Inc., New York, USA, 1991.
- [2] The Temperature Ratings of Electronic Parts, Design, Materials, compounds, Adhesives, Substrates, Number1, Semiconductor, Test & Measurement. 10 (2004). <https://www.electronics-cooling.com/2004/02/the-temperature-ratings-of-electronic-parts>
- [3] Lloyd Condra, Diganta Das, Neeraj Pendse and G.Pecht, Junction Temperature Considerations in Evaluating Electronic Parts for use Outside Manufacturers-Specified Temperature Ranges, *IEEE Transactions on Components and Packaging Technologies*. 24 (4) (2001) 721-728.
- [4] Su Jingxin, M.Ma, T.Wang, X.Guo, L.Hou, and Z.Wang, Fouling corrosion in aluminum heat exchangers, *Chinese Journal of Aeronautics*. 28 (3) (2015) 954–960.
- [5] F. Sarvar, D. Whalley, and P. Conway, Thermal Interface Materials - A Review of the State of the Art, *1st Electronic System integration Technology Conference*. 2 (2006) 1292–1302.
- [6] K.E.starner and H.N.McManus, An Experimental Investigation of Free-Convection of Heat Transfer From Rectangular-Fin Arrays, *Journal of Heat Transfer*. 85 (3) (1963) 273–277.
- [7] Charles D. Jones and Lester F. Smith, Optimum Arrangement of Rectangular Fins on Horizontal Surfaces for Free-Convection Heat Transfer, *Journal of Heat Transfer*. 92 (1) (1970) 6-10.
- [8] H. Y. Li and S. M. Chao, Measurement of performance of plate-fin heat sinks with cross low cooling, *International Journal of Heat and Mass Transfer*. 52 (2009) 2949–2955.
- [9] C. J. Kobus and T. Oshio, Development of a theoretical model for predicting the thermal performance characteristics of a vertical pin-fin array heat sink under combined forced and natural convection with impinging flow, *International Journal of Heat and Mass Transfer*. 48 (6) (2005) 1053–1063.
- [10] R. Ricci and S. Montelpare, An experimental IR thermo graphic method for the evaluation of the heat transfer coefficient of liquid-cooled short pin fins arranged in line, *Experimental Thermal and Fluid Science*. 30 (4) (2006) 381–391.

- [11] N. Sahiti, F. Durst, and P. Geremia, Selection and optimization of pin cross-sections for electronics cooling, *Applied Thermal Engineering*. 27 (1) (2007) 111–119.
- [12] S. Shanmugan and D. Mutharasu, Thermal Resistance Analysis of High Power Light Emitting Diode Using Aluminum Nitride Thin Film-Coated Copper Substrates as Heat Sink, *Journal of Electronic Packaging*. 136 (3) (2014) 34502 (1-6).
- [13] L. J. Schowalter, G. A. Slack, J. B. Whitlock, K. Morgan, S. B. Schujman, B. Raghothamachar, M. Dudley, and K. R. Evans, Fabrication of native, single-crystal AlN substrates, *Physica Status Solidi C: Conferences*. (7) (2003) 1997–2000.
- [14] C. R. Dietz and Y. K. Joshi, Single-Phase Forced Convection in Microchannels with Carbon Nanotubes for Electronics Cooling Applications, *Nanoscale and Microscale Thermophysical Engineering*. 12 (3) (2008) 251–271.
- [15] R. Senthilkumar, S. Prabhu, and M. Cheralathan, Experimental investigation on carbon nanotubes coated brass rectangular extended surfaces, *Applied Thermal Engineering*. 50(1)(2013)1361–1368.
- [16] R. Senthilkumar, A.J.D. Nandhakumar, and S. Prabhu, Analysis of natural convective heat transfer of nano coated aluminum fins using Taguchi method, *Heat and Mass Transfer*. 49 (1) (2012) 55–64.
- [17] Z. Yao, Y. Lu, and S.G. Kandlikar, Micro/Nano Hierarchical Structure in Micro channel Heat Sink for Boiling Enhancement, *MEMS, IEEE*, (2012) 285–288.
- [18] H. Lotfizadeh, A. Abouei, M. Sanagoo, and S. Rezazadeh, Thermal performance of an innovative heat sink using metallic foams and aluminum nanoparticles — Experimental study ☆, *International communication in Heat and Mass Transfer*. 66 (2015) 226–232.
- [19] M. Yakut Ali, F. Yang, R. Fang, C. Li, and J. Khan, Thermo hydraulic characteristics of a single-phase micro channel heat sink coated with copper nanowires, *Frontiers in Heat and Mass Transfer*. 2(3) (2011) 1-11.
- [20] Antonios I. Zografos and J. Edward Sunderland, Natural convection from pin fin arrays, *Experimental Thermal and Fluid Science*. 3(4) (1990) 440-449B.
- [21] Y. Joo and S. J. Kim, Comparison of thermal performance between pate-fin and pin-fin heat sinks in natural convection, *International Journal of Heat and Mass Transfer*. 83 (2015) 345-356.
- [22] Strupstad A. Error Analysis of Flow Experiments, Trondheim, 2009.